7-12-2009

Developing Abrasion Test Standards for Evaluating Lunar Construction Materials

Ryan L. Kobrick
University of Colorado Boulder, kobrickr@erau.edu

David M. Klaus
University of Colorado Boulder

Kenneth W. Street
NASA Glenn Research Center

Scholarly Commons Citation

Kobrick, R. L., Klaus, D. M., & Street, K. W. (2009). Developing Abrasion Test Standards for Evaluating Lunar Construction Materials. *SAE International Journal of Aerospace, 4*(1). https://doi.org/10.4271/2009-01-2377

2009-01-2377

Developing Abrasion Test Standards for Evaluating Lunar Construction Materials

Ryan L. Kobrick and David M. Klaus
University of Colorado at Boulder

Kenneth W. Street
NASA Glenn Research Center

ABSTRACT

Operational issues encountered by Apollo astronauts relating to lunar dust were catalogued, including material abrasion that resulted in scratches and wear on spacesuit components, ultimately impacting visibility, joint mobility and pressure retention. Standard methods are being developed to measure abrasive wear on candidate construction materials to be used for spacesuits, spacecraft, and robotics. Calibration tests were conducted using a standard diamond stylus scratch tip on the common spacecraft structure aluminum, Al 6061-T6. Custom tips were fabricated from terrestrial counterparts of lunar minerals for scratching Al 6061-T6 and comparing to standard diamond scratches. Considerations are offered for how to apply standards when selecting materials and developing dust mitigation strategies for lunar architecture elements.

INTRODUCTION

The Vision for Space Exploration (VSE), announced in 2004, refocused NASA's direction to "undertake lunar exploration activities to enable sustained human and robotic exploration of Mars and more distant destinations in the solar system" [1]. The VSE then led to the NASA Authorization Act of 2005, calling for a "sustained human presence on the Moon". Before humankind returns to its nearest celestial body, however, research is needed to better understand many characteristics of the Moon, and in particular, lunar dust, which caused numerous problems for the crew and hardware on the six Apollo surface missions. While astronaut safety concerns are the top priority, dust mitigation will also be needed for other surface elements of the lunar architecture, including the Lunar Lander *Altair*, Extravehicular Activity (EVA) Systems (EVAS), crew surface mobility aids and robotic systems. NASA's Global Exploration Strategy (GES) is the blueprint for implementing the VSE. Under the theme of Exploration Preparation, one of the highlighted objectives presented at AIAA's 2nd Space Exploration Conference (Houston, TX, 2006), was to "evaluate and employ dust mitigation techniques to protect crews, materials, and instruments during extended surface stays" [2]. As further explained by Tony Lavoie, this will be critical to test technical capabilities, and characterize critical environmental parameters and lunar resources. The GES also led to the announcement of the Lunar Architecture Team (LAT) who released two reports on defining lunar objectives. In the fall of 2007, the Constellation Architecture Team-Lunar (CxAT-Lunar) was formed to investigate the transportation elements of future missions [3]. Then, per the results and assessment of the Exploration Systems Architecture Study, the Dust Management Project (DMP) was created in NASA's Exploration Technology Development Program. Implementation of the DMP continues to be refined by the results of follow on NASA studies and technology needs assessments for the Constellation Program. The DMP has investigators spread across different centers, industries and universities, and is structured into four main branches including Engineering Design Environment, Technology Development, Technology Integration and Testing, and Education and Outreach. The abrasion work presented here falls under the first branch in the areas of Regolith Characterization and Simulant Development and Characterization.

BACKGROUND

A detailed characterization of the lunar environment and a review of abrasion theory were described in a paper presented at the International Astronautical Congress, 2008, Glasgow, UK [4]. Select information is summarized in this paper.

APOLLO ERA

Gaier [5] cataloged the specific effects of lunar dust on EVAS during the Apollo era and additionally noted that the severity of dust problems was consistently underestimated by ground tests. Points of concern for astronauts on lunar EVA included issues such as vision obscuration, false instrument readings, dust coating and contamination, loss of traction, clogging of mechanisms, abrasion, thermal control problems, seal failures, inhalation and irritation, excessive crew time being used to clean EVA suits and equipment, and electrical conductivity. Problems plagued the entire mission from before touchdown, when jet-blasted dust impeded vision and led to a landing that straddled a crater, to continuous eye irritation on the return trip to earth. Dust abrasion problems that are specific to this research included:

- Conrad and Bean's suits were worn through above the boot, including Micrometeoroid protection layer and several layers of Kapton® multi-layer thermal insulation were breached
- Wear noted on outer layer of Mylar® multi-layer insulation on boots
- Pressure integrity failures
- Gauge dials scratched (Lunar Roving Vehicle (LRV) unreadable on Apollo 16) and pitted
- Harrison Schmitt's visor sunshade so scratched he could not see in certain directions (Apollo 17)
- Apollo 17 astronaut glove covers were worn through after drilling cores on two (of three) EVA excursions

DUST IN THE LUNAR ENVIRONMENT

Understanding the dynamics of the lunar environment is essential to being able to characterize the forces and variables that can affect lunar dust transport and material abrasion. Lunar soil primarily results from innumerable micrometeorite impacts forming everything from spheres to highly angular and irregular shape silicate glass particles [6]. Pulverization of the lunar materials creates small particles or causes agglutinate formation to occur which forms large particles or conglomerates (or impact breccias). Pulverization can also completely melt the materials forming glass [7]. This process causes some mixing from region to region on the Moon, but in the absence of an atmosphere or any form of erosion or fluid motion, the particles are not sorted by size and they maintain their abrasive properties. Lunar dust less than 20 μm accounts for 10-20% of the regolith's bulk mass [6]. NASA's Constellation program uses a definition of less than 10 μm for dust [8], while the DMP in NASA's Exploration Technology Development Project has heretofore been using 20 μm. Traditionally the Moon is categorized into two distinct regions: the basaltic-rich mare and the anorthositic highlands. The regolith is deeper in the older highlands than the maria. The maria contain dark basalts, while the lunar highlands have lighter-colored feldspar-rich rocks [9]. For abrasion considerations, the region where exploration will take place will dictate the type of dust particle interactions on hardware. Other environmental considerations for abrasion testing include:

- Relative micrometeorite bombardment (distributed approx. by power law, sizes ranging 30-150 μm in radius, masses of 10^{-10} to 10^{-8} kg, and impact at speeds averaging 7 km/s) [9], the "backside" of the Moon experiences a higher rate of micrometeorite impacts
- Earth-Moon orbital alignment with respect to the Sun
  - Temperature (40 Kelvin - 396 Kelvin) [10]
  - Electrostatic charging via photoelectric effects
  - Radiation
- Lunar gravity (mean equatorial force 1.62 m/s^2) [10]
- Near vacuum (approx. 10^{-14} torr)
- Absence of humidity
- Chemical reactivity (within exposed air systems) [11]

The properties and composition of dust particles of less than 20 μm are not well known, as this portion of returned lunar samples was not well preserved, partially because the dust grains in that range tended to adhere to the sample bags and were not removed for analysis. Relative density increases with regolith depth, suggesting that the regolith becomes more compact the further down it occurs [9]. Because of the properties of density, void ratio, cohesion, and friction angles, crater rims are expected to be less dense (less than 50%) than the surrounding lunar terrain [9]. This is important to note for exploration activity, as it may result in more dust leaving the surface as well as greater penetration of hardware into the soil. Regolith density from actual missions was found to be higher than predicted, and the increase with depth was suggested to be primarily due to self-weight. Density estimations and calculations suggest that the soil on slopes is considerably less stable [12].

ABRASION THEORY / HARDNESS

The lunar science community identified the abrasive nature of lunar dust as one of the top five physical properties of interest. Abrasion's importance was ranked as 'high' because it affects any material that moves or has a sealing surface. In the field of Tribology, abrasion is one of the four basic types of wear or physical mechanisms for material removal or displacement [13]

and is the most severe and most costly form of wear [14]. Wear is not a basic material property, but a system response of the material as a function of its use [13]. Abrasive wear occurs when a hard protuberance (asperity) on the surface of a material, or a hard, loose particle trapped between surfaces, plastically deforms, gouges or cuts the counter surface as a result of motion. The result is a series of grooves in soft material or surface fractures in brittle material. Additionally, with hard material this is often accompanied by the resulting formation of wear particles. Abrasion can be sub-categorized by degree of freedom into two tribosystems; two-body and three-body wear. Two-Body abrasive wear occurs when hard particles or protuberances, which produce the wear of one body, are fixed on the surface of the opposing body [15]. A simplified example would be sandpaper against a surface. Three-Body abrasive wear occurs when loose particles are introduced or generated between the contacting surfaces [15]. For example, this occurs when sand is continually poured between two plates rubbing against each other. Two-body fixed abrasives are typically used for testing plastics, metals, ceramics, and composites, while 3-body testing is used for all materials [14].

Degree of freedom influences the abrasiveness of a test, and generically two-body abrasion will produce significantly higher wear than three-body, because three-body particles have the ability to roll. This may make two-body measurement easier to obtain since the wear would be more sizeable. The wear on a material is fairly constant when the abrasive is much harder than the material. For this reason, the material property of hardness can be used as an estimate of how much abrasion is expected between a pair of materials.

Hardness is the resistance to plastic deformation. The traditional and earliest quantifiable method of measuring hardness is by a scratch test, which compares the ability of the substance to scratch or be scratched by a series of standard minerals. With several standard tests methods available, lunar dust hardness can be approximated (see Figure 1 for scale comparison and commonly used or proposed space construction materials). In passing, it should be noted that hardness ranges occur for minerals due to compositional variation (e.g., Diamond) and crystal orientation (e.g., Apatite).

A wear coefficient, k, can be determined by measuring the wear volume after an abrasive test and knowing the load used, the sliding distance, and the hardness of the softer material as seen in Equation 1 [15] (Note, when calculating k, the wear volume divided by the sliding distance is the average cross sectional wear area).

$$\text{wear volume} = k\left(\frac{\text{load} \times \text{sliding distance}}{\text{hardness of softer material}}\right) \quad \{1\}$$

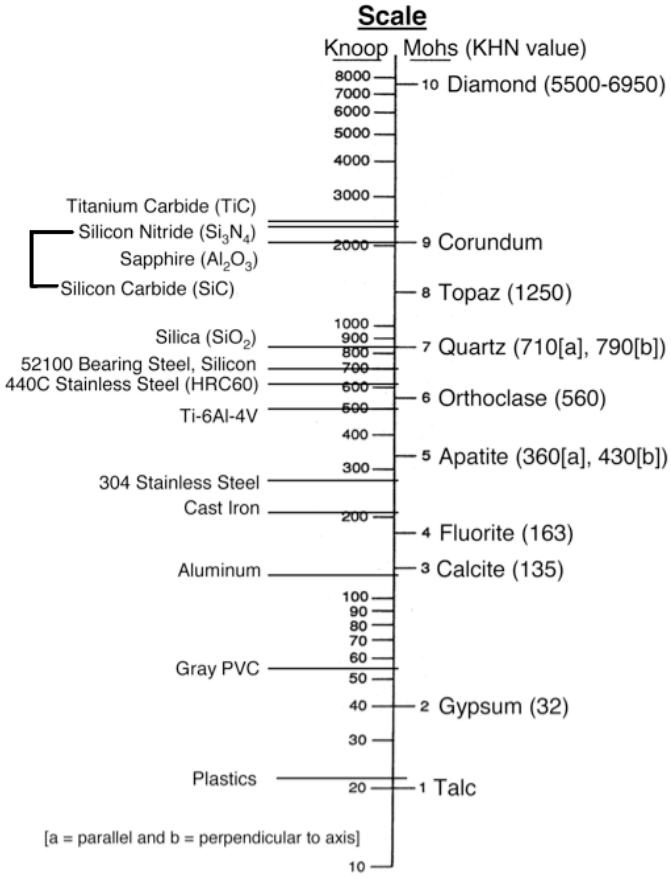

Figure 1. Comparison of Mohs to Knoop hardness [7] with typical spacecraft materials

When the material and abrasive hardness's are similar, the interactions approach polishing, and wear resistance improves by an order of magnitude. Since the wear coefficients for these materials would be similar, Equation 1 would no longer be valid. The k-value for abrasion relates to the sharpness, or geometry, of the asperity or particle causing the wear. Equation 1 is the simplest form of the wear equation, where k also physically represents the average tangent of the roughness angle divided by π [16] as seen in Figure 2. In Figure 2, the abrasive grain removes material from a bearing surface over a distance of x.

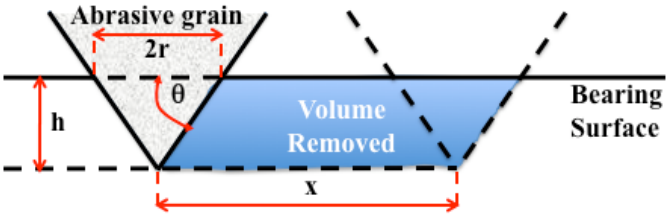

Figure 2. Simplified abrasive wear model showing how a cone removes material from a surface [adapted from 16]

ASTM Standard G 171-03 [17] specifies calculating a Scratch Hardness Number, HS_P (Pa), based on applied normal load, P (N), and scratch width, w (m) as shown in Equation 2.

$$HS_P = \frac{8P}{\pi w^2} \quad \{2\}$$

This relationship assumes a hemispherically-tipped stylus that produces a groove whose leading surface has a radius of curvature, R, the tip radius of the stylus. The projected area of the contact surface is a semi-circle with diameter equal to the scratch width [17]. With scratches on the order of microns, expected values of HS_p are in the GPa range.

The two main failure modes relating to hardness were noted by Rickman and Street [7] as occurring along preferential orientations controlled by crystallography or independent of orientation. These failure modes can then be related to the abundant lunar minerals and how conchoidal fractures occur in minerals and glass creating sharp, serrated edges or highly angular (pointed) tips. The crystal orientation relating lunar mineral shape formation to hardness and then to abrasion will be further investigated. Another observation was that two minerals with similar hardness values but different toughness values (ability to absorb mechanical or kinetic energy up to failure) produced different wear levels.

For nonmetallic materials, hardness is also affected by relative humidity [18]. Westbrook and Jorgensen showed that micro-hardness was lowered by absorbed water, but confined to a region not more than 3 μm from the free surface. In addition, hardness can change with depth of penetration from the surface [19]. Since scratching depth can be estimated by 1/10th of a particles diameter, a particle with a diameter larger than 30 μm would scratch below the absorbed water region of a nonmetallic material. In the lunar regolith, 10-20% of the particles are finer than 20 μm with an unaccounted for hardness [6, 8]. Multiple scratches from dust can penetrate surface coatings and treatments, while larger particles could penetrate a coating in a single scratch.

Figure 3. CSM Revetest Scratch tester with glovebox enclosure for humidity reduction

TWO-BODY SCRATCH TESTING

In order to investigate the fundamental science of material interactions, a two-body scratch test was determined to be the most efficient apparatus. The American Society for Testing and Materials (ASTM) standard G 171-03 [17] prescribes using a diamond tipped stylus with a constant normal load with recommendations for speed of travel. The CSM Revetest Scratch Tester (see Figure 3) was used with a 200 μm radius diamond tip with 120˚ angle to acquire baseline scratch data on commonly used aluminum alloy, Al 6061-T6 (see Figure 4). Al 6061-T6 was chosen as the initial testing phase material for the following reasons.

- Al 6061-T6 is commonly used in space structures
- Al 6061-T6 has well documented material properties
- It is known that the abrasives will wear the material in a measurable amount

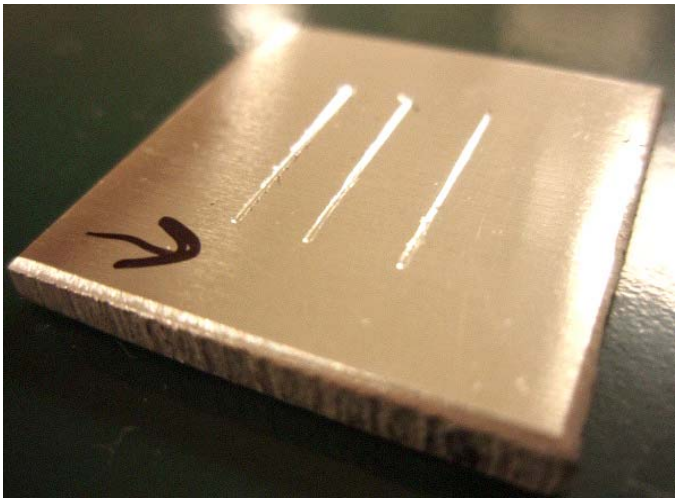

Figure 4. Specimen of Al 6061 T6 with three scratches

The spherical tip of the diamond indenter allows for theoretical width measurement, 2 x a, to be calculated from the semi-angle of the apex, θ, tip radius, R, and scratch depth, δ_P (see trigonometry formulas in Equation 3 [20] and Figure 5). This dimensionality can be expanded to custom shaped tips and will be investigated in this research effort.

$$\begin{aligned} \delta_S &= R(1-\sin\theta) \\ \phi &= \cos^{-1}(1-\delta_P/R), \quad \text{for } \delta_P \le \delta_S \\ a &= R\sin\phi, \quad \text{for } \delta_P \le \delta_S \\ a &= R\cos\theta + (\delta_P - \delta_S)\tan\theta, \quad \text{for } \delta_P > \delta_S \end{aligned} \quad \{3\}$$

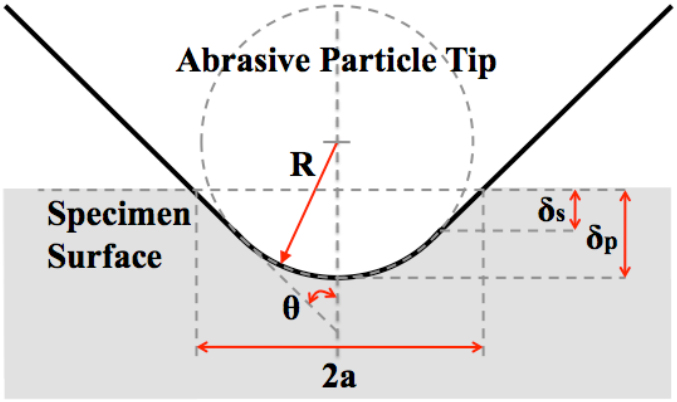

Figure 5. Spherical geometry of abrasive particle tip

LUNAR MINERALOGY

A diamond tip is useful for acquiring baseline scratch data on anticipated space hardware construction materials (examples shown in Figure 1), but it does not represent any mineral commonly found in the lunar environment. To investigate this issue, it was determined that it would be best to fabricate custom scratch tips made out of lunar minerals and then compare results to the diamond scratch data.

Table 1 lists the significant lunar minerals, their Mohs hardness values, the percentage abundance (A-abundant, M-major, m-minor, t-trace), and chemical composition. These parameters were used in the criteria for selecting minerals for tips. Anorthite and enstatite are ideal candidate materials because of their lunar abundance. Labradorite could be tested because of its hardness and abundance, making it a potential worst-case scenario for abrasive wear on the Moon. It would be desired to also use hercynite or spinel, but the low abundance suggests that the interactions with construction materials would be small unless an engineering process concentrates these materials. Ideally as we collect data from the Moon in future missions, abundance and concentrating processes can be quantitatively addressed.

Using the base ingredients of the NU-LHT simulant, anorthosite was used to create a custom tip. Anorthosite is 90% rich plagioclase feldspar and the composition is largely composed of labradorite. Figure 6 shows an optical photograph of a custom anorthosite tip embedded in epoxy before being used for trial scratches. The approximate dimensions are 3.4 mm in base length (base not fully shown), 2.5 mm in height (from base to tip), and 1.0 mm thick. This tip was used as a demonstration and future tests will document tip geometry for comparison to diamond stylus data.

Table 1. Significant Lunar Minerals [Adapted from 7]

Mineral	Mohs	%	Chemical Composition
Anorthite	6	A	$CaAl_2Si_2O_8$
Bytownite	6.0-6.5	M	$(Ca,Na)(Si,Al)_4O_8$
Labradorite	7	M	$(Ca,Na)(Si,Al)_4O_8$
Olivine	6.5-7.0	M	$(Mg,Fe)_2SiO_4$
Fayalite	6.5-7.0	-	Fe_2SiO_4
Forsterite	6.5-7.0	-	Mg_2SiO_4
Clinoenstatite	5.0-6.0	M	$Mg_2[Si_2O_6]$
Pigeonite	6	M	$(Mg,Fe^{+2},Ca)_2[Si_2O_6]$
Hedenbergite	6	M	$CaFe^{+2}[Si_2O_6]$
Augite	5.5-6.0	M	$(Ca,Na)(Mg,Fe,Al,Ti)[(Si,Al)_2O_6]$
Enstatite	5.0-6.0	A	$Mg_2[Si_2O_6]$
Spinel	7.5-8.0	m	$MgAl_2O_4$
Hercynite	7.5-8	m	$Fe^{+2}Al_2O_4$
Ulvospinel	5.5-6.0	m	$TiFe^{+2}{}_2O_4$
Chromite	5.5	m	$Fe^{+2}Cr_2O_4$
Troilite	4	t	FeS
Whitlockite	5	t	$Ca_9(Mg,Fe^{+2})(PO_4)_6(PO_3OH)$
Apatite	5	t	$Ca_5(PO_4)_3(OH,F,Cl)$
Ilmenite	5.5	m	$Fe^{+2}TiO_3$
Native Iron	4.5	t	Fe

%: A-abundant, M-major, m-minor, t-trace

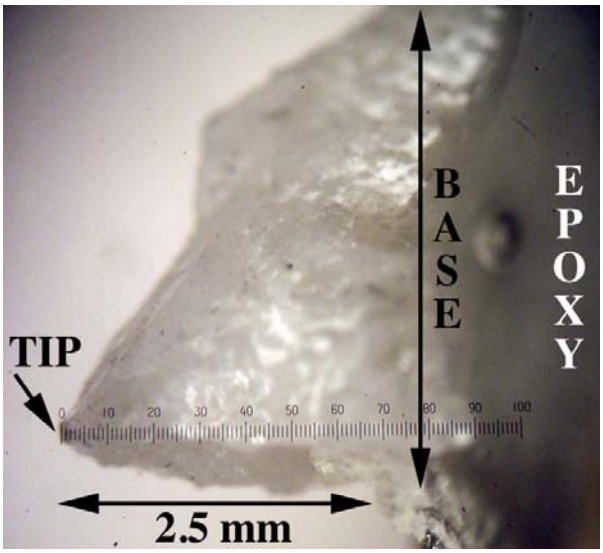

Figure 6. Custom anorthositic tip, 40x magnification embedded in epoxy (photographed at NASA GRC by R.L. Kobrick)

ABRASIVE WEAR MEASUREMENTS

Abrasive wear can be measured in terms of linear change (like the length of a pin), by area change, or volume change. These changes relate to a change in mass and can be measured with varying accuracy. Displacement and deformation of material must also be measured or analyzed when quantifying the amount of wear since they will not have an associated mass loss and may create other asperities. Surface displacement or distress can be measured with optical microscopy by examining characteristics like the surface roughness or if cracking is present. These measurements are also dependent on other variables such as time required. Another method to measure the amount of abrasive wear is by the change in reflectance, which was used on the Wheel Abrasion Experiment on the Mars Pathfinder's deployable rover Sojourner [4]. Examples of where linear wear occurs include bushings or shafts, ball-bearing retainers, sliding actuator parts, and piston-cylinder wall contacts. An example of an area change is when a stationary block is abraded on a rotating ring [13]. Volume wear is more common in testing because scars can usually not be simplified in two-dimensions.

For large amounts of wear, mass loss can be used as a fairly accurate indicator, but does not account for the material displacement. Smaller amounts of wear become more expensive to measure since sensitive equipment is needed to detect minute changes. Volume loss can be difficult to measure for both large and small amounts of wear because irregular scar shapes are developed. Measuring wear with respect to time is a common practice and a wear-time ratio can be defined as wear velocity measured in millimeters/minute (mm/min) [13]. Wear effectiveness can be defined as the wear rate (mm/min) divided by the friction force (N) [21]. ASTM standards typically use volume differences because materials with different densities can be directly compared (cubic millimeters). Another mass loss rate in use is fractional change in mass (for e.g., 1% change per 100 hours of operation).

The following is a summary of the parameters influencing wear adapted from references 13, and 21.

- Material parameters: composition, density, grain size, reciprocated shape factor (defined as: perimeter^2 / 4π x area), spike parameter (Hamblin's numerical descriptor to characterize abrasiveness of particle geometry), modulus, thermal conductivity, degree of work hardening, and hardness
- Design parameters: shape, loading, type of motion, roughness, vibration, and cycle time
- Environmental parameters: temperature, humidity, atmosphere, and contamination
- Lubrication parameters: type of lubricant, lubricant stability, and type of fluid lubrication
- Wear-in: Presence or absence (the break-in cycle associated with the start of a test)

The ASTM documentation provides recommended steps for selection of a test configuration and structural parameters [13]. These guidelines were used in defining appropriate tests to be conducted for lunar dust abrasion experiments.

EXPERIMENTAL OVERVIEW

The experimental methodology and test approach are described in a paper presented at the International Astronautical Congress, 2008, Glasgow, UK [4], which follow ASTM Standard G 171-03 [17] as a guide. A total of 36 scratches were made using a standard diamond tip (200 μm radius, 120˚ apex angle) in Al 6061-T6 at constant normal loads of 5, 10, 15, 20, 40, and 60 N. 3 scratches were made at each load against the striations on the surface finish of aluminum and 3 with the surface finish. A custom anorthositic tip was fabricated (Figure 6) and 12 scratches were made all against the surface finish direction. Three scratches were made at constant normal loads of 5, 10, and 15 N and one scratch per 20, 40, and 60 N normal load was made. The anorthositic tip was photographed before the tests but geometrical analysis was not conducted, as this tip was a proof of concept demonstration.

Each scratch was imaged with the Veeco NT100633 Optical Surface Profiler (Veeco) at three locations (see Figure 7) for measurement analysis.

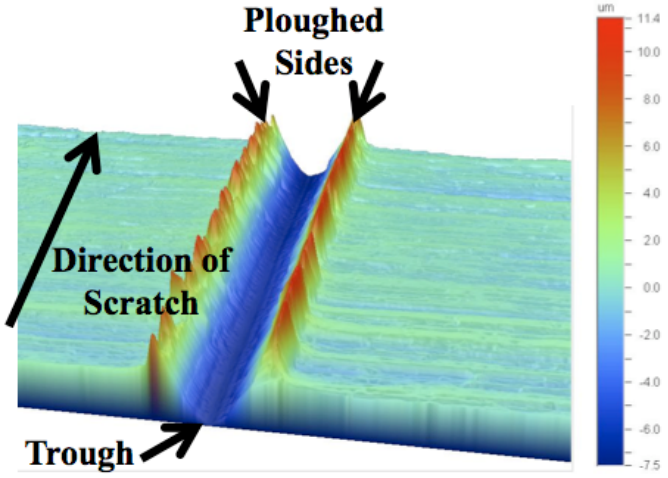

Figure 7. 3-D profile of diamond tip scratch on Al 6061-T6 with 10 N normal load against the striations on the surface finish (Scale is -7.5 to 11.4 μm)

The Al 6061-T6 samples scratched with the diamond tip underwent a Rockwell Hardness Test (HRB) using a steel ball indenter with a 1.5875 mm (1/16") diameter with a test force of 980.7 N (100 kgf). A dwell loading time of 10 seconds was selected with a dwell reading time of 2 seconds. The average HRB value was 57.3 ± 0.6 from 12 samples with 5 readings each. This corresponds well with the metals handbook [22], which

estimates a HRB value of 60.0 converted from the Brinell Hardness Value of 95.0.

Scanning Electron Microscopy (SEM) was conducted on the diamond scratched surfaces to investigate the surface morphology (see Figure 8).

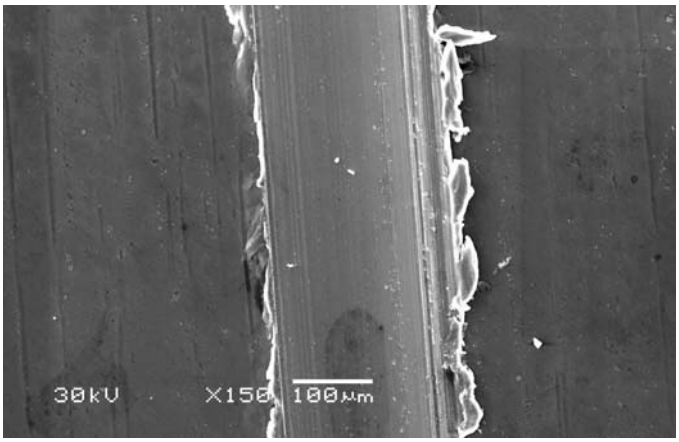

Figure 8. SEM image of scratch formed with constant normal load of 40 N (CU-Boulder by Prof. Sayed Khalil)

The principle difference in methodology for the standard diamond tip versus a custom tip is the constant imaging that is needed to observe the geometrical changes of the custom tip that occur due to the imperfections in the crystal structures.

MEASUREMENT STANDARDS

This section of the paper addresses shortcomings of current standards as applicable to our needs and presents preliminary data from scratch profiles obtained.

MATLAB CODE DEVELOPMENT

The ASTM Standard G 171-03 specifies that at least three width measurements should be made on each scratch, but by taking an entire profile with an optical profiler, statistically sound measurements can be calculated. Each Veeco profile that was recorded contained a grid of 736 by 480 X, Y (surface location in scan), and Z (height) coordinates (353,280 data points). This means that up to 1,440 width profiles can be measured with three Veeco scans, which is statistically more valid than the recommended amount of three. In order to analyze the large data sets two approaches were used. The first employed Excel, but it could only handle individual cross sections taken from the Veeco software and not the total scratch array. This limitation along with the manual data searching for critical points, like scratch width end points, was the motivation for developing a code in MATLAB that could manipulate all of the 3D-profile data. The University of Colorado at Boulder (CU-Boulder) license was provided by The MathWorks Inc.

The first propagated error that needed to be removed by the MATLAB code was that profiles taken in the Veeco had a false zero baseline value. This occurred because of the scratch in the profile caused the instrument to think the zero value was within the average of the entire profile. This offset data was used to adjust each profile to a true zero value or “Zero Line” location. This was found by averaging the height values to the left of each scratch, away from the deformation zone (shown in Figure 9). Data that were removed included any points with an error on a given height measurement (could be caused by sharp edge reflections) and width measurements with negative values and outliers according to Chauvenet’s Criterion of statistical rejection [23] (with 480 width measurements in each profile outliers existed). This code could be applied to any input data with three dimension and outputs key measurements of scratch width, scratch depth, area removed, and ploughed area. These values lead to abrasion calculations of various coefficients like the wear coefficient and scratch hardness number previously mentioned and a cut-to-plough ratio (not included in this paper).

SCRATCH WIDTH STANDARDIZATION

A limitation to the ASTM Standard G 171-03 [17] for width measurement is that a specific location on the scratch trough is not specified. Average width is determined by visual inspection. With today’s technology, the standard could be updated to include the use of a surface profiler and a code such as the one developed for this research. For consistency a scratch width location within a profile cross section would need to be determined. For this research, the scratch width was defined as the location within the scratch trough at the Zero Line (as shown in Figure 9). Figure 9 also shows how a single cross-section profile is not sufficient if the surface is not perfectly flat or if it has a tilt.

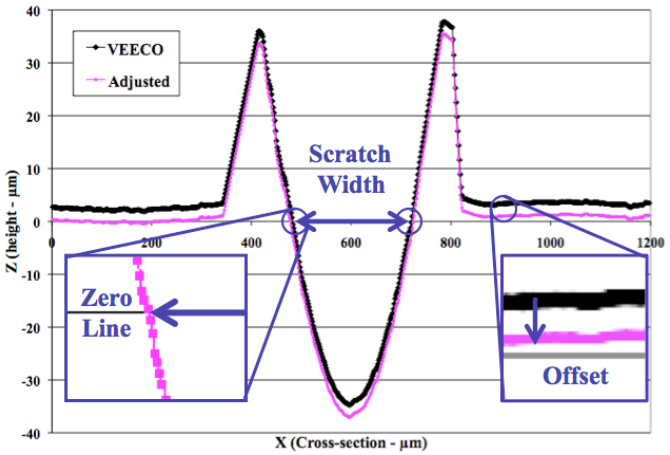

Figure 9. Standardizing scratch width location and offset

MEASUREMENT CONFIDENCE INTERVAL

Since a given sample will have a unique surface roughness (Ra), the Zero Line from a dataset will rest on the top surface of this measurement. To establish a confidence interval of the width measurement, a standard deviation equal to the Ra was used above and below the Zero Line to shift the data for width analysis (as seen in Figure 10). If the Ra is small, then the entire scratch profile will shift below the Zero Line making the change in the measurements negligible.

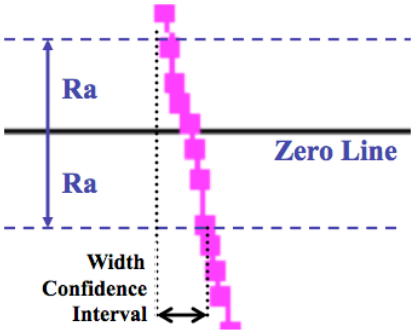

Figure 10. Left hand side of scratch data showing confidence interval using surface roughness (Ra)

The Ra values for the samples were averaged over the area to the left of each scratch within the Veeco profiles. The average Ra on the samples was 0.35 ± 0.18 µm and the frequency distribution is shown in Figure 11.

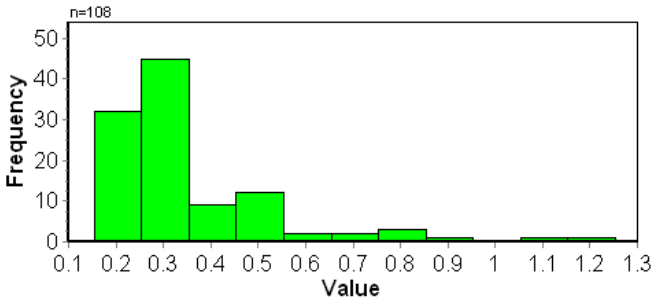

Figure 11. Surface roughness distribution in µm (12 Al 6061-T6 samples with 108 profiles)

When scratches occur, the Ra of a given material will change. This can impact functionality and lead to system failures. For example, on a profile with a 60 N normal load scratch, the Ra changes from the baseline 0.3 µm to 10 µm. This drastic change occurs because of the depth and width of the scratch coupled with the height and inconsistency of the ploughed material. The ploughed material analysis is not reported in this paper.

PRELIMINARY DATA ANALYSIS

The following section presents preliminary data from the two-body abrasion scratch tests. It should be noted that outliers have not been removed at his stage in the research and that curve fit equations are included to visually show the approximate mean values with outliers. Future plots will remove outliers and include statistical analysis with correlation coefficients.

ERROR ANALYSIS

Scratches conducted with a diamond tip were conducted both against and with the surface finish striation direction of the Al 6061-T6. Figure 12 shows that the principle measurements of width and depth show negligible difference between the two variations in surface finish direction. There are more outliers present in this data set for scratches made against the surface finish direction. This does not suggest that a scratching trend in the direction of the finish is desired and either direction yields similar results. Scratch area removed, total ploughed area, and volume removed data is not discussed in this paper.

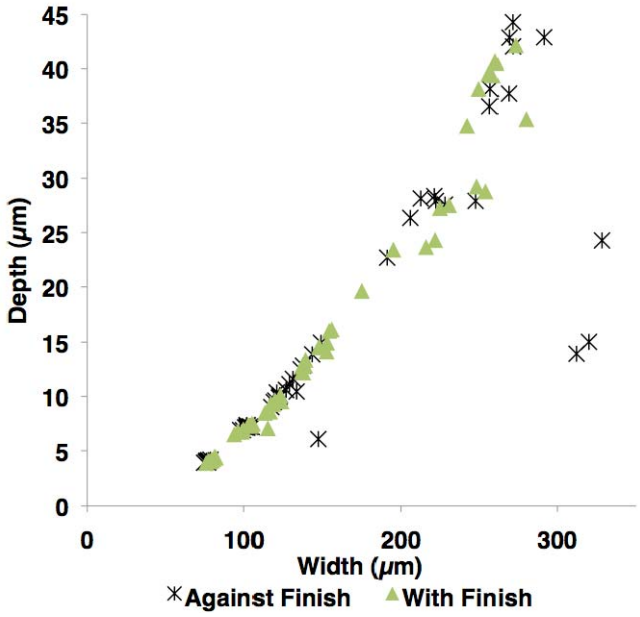

Figure 12. Scratches made with and against the surface finish striations (18 scratches, 54 profiles each direction)

Figure 13 shows 6 scratches that were made with a similar constant normal load setting. The included error bars are only for the Zero Line data. The load values were averaged from 23 to 80 seconds during the scratch test time (avoiding the initialization and loading times) and standard deviations were calculated. The average load deviation for these scratches was found to be ±0.1 N. This is consistent with other load values. Also shown in Figure 13 are the width measurements with standard deviations for the Zero Line data with widths if the data was shifted by the Ra either up or down (Minus/Plus Ra). The error induced by the uncertainty of the Ra is less than the standard deviations of the width measurements. This implies for the Ra finish of the Al 6061-T6 samples, the Zero Line used to measure data for all profile loads is statistically correct even with the roughness uncertainty.

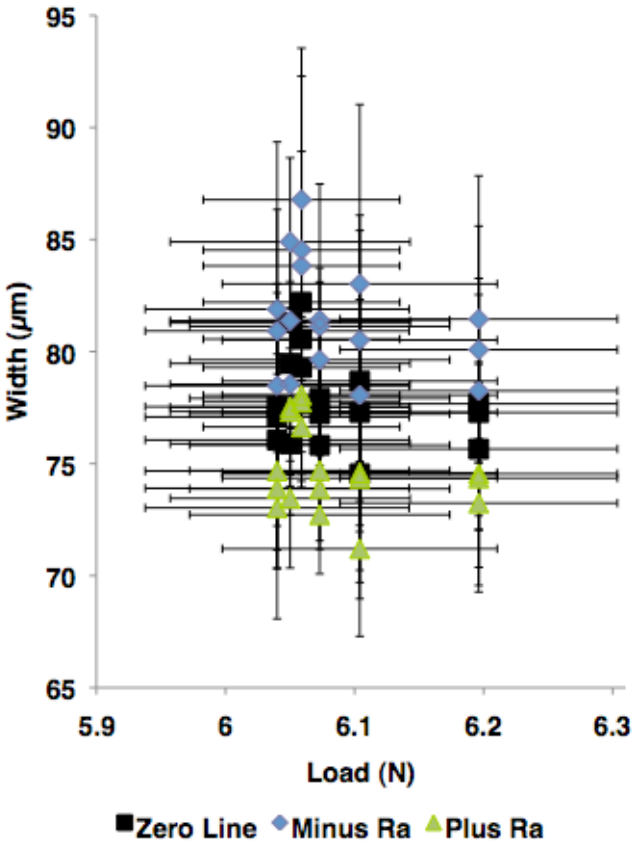

Figure 13. Scratch width versus load (6 scratches, 18 Profiles) showing standard deviations

KEY MEASUREMENTS FOR TWO-BODY ABRASIVE WEAR

In Figure 14 we see that the diamond tip scratch measurements for width and depth match the theoretical calculations for a sphere tip. This comparison could be expanded to integrate the theoretical area (or volume) displacement in the scratch trough to compare to measured data. This exercise will be conducted in future analysis. The custom anorthositic tip data is also included in this figure to show the diversity of measurements that were made. Since this tip was a proof of concept, there is no geometry data to compare with. Ideally a relationship between tip hardness, geometry and scratch area removal can be established. This is conducted by taking tip images through a microscope before and after scratches to measure any changes. This can be used to predict theoretical width-depth measurements.

As seen in Figure 15, as the load was increased using the diamond tip, the scratch width measurements have a greater range of values. This needs to be further investigated to determine whether this is an artifact of material removal.

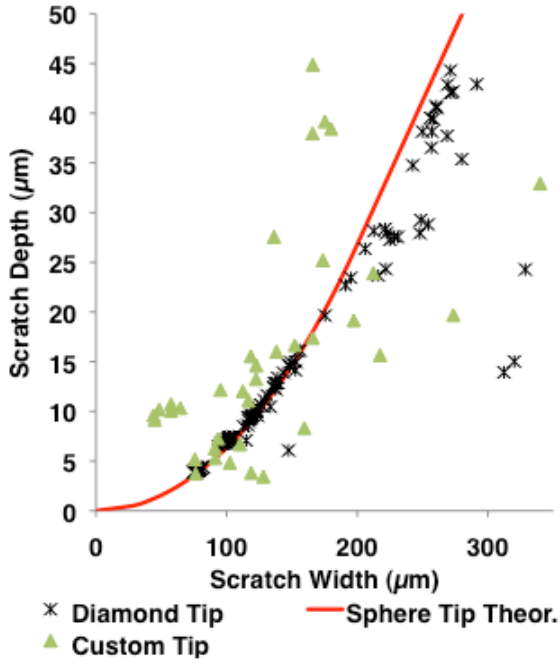

Figure 14. Data from diamond tip (36 scratches, 108 profiles) and custom anorthositic tip (12 scratches, 36 profiles) with theoretical sphere tip data of width versus depth

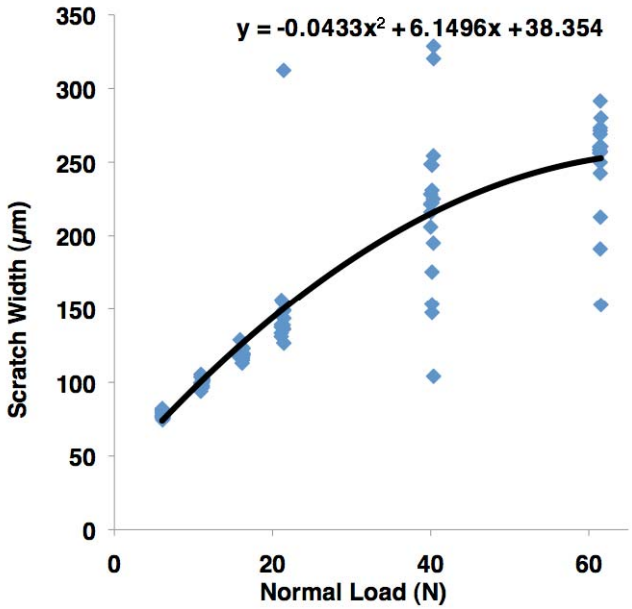

Figure 15. Scratch width versus normal load (36 scratches, 108 profiles)

Figure 16 and Figure 17 show the basic wear coefficient and scratch hardness number plotted as a function of normal applied load using a diamond tip. The wear coefficient increases with load while the scratch hardness number remains fairly consistent between 2 and 3 GPa.

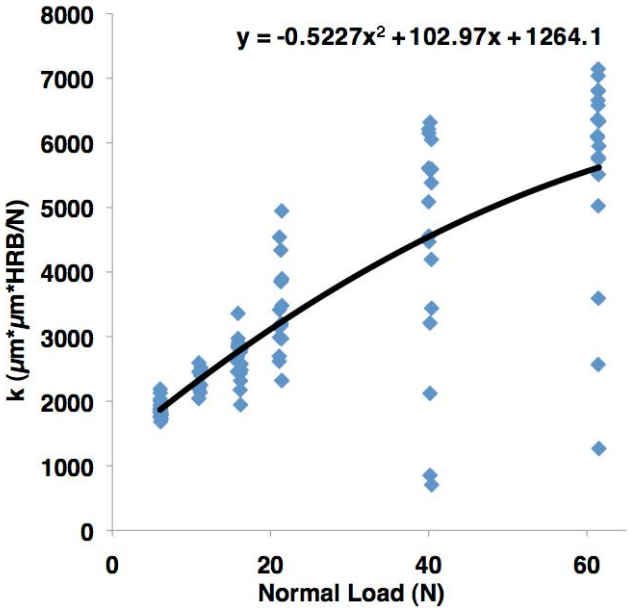

Figure 16. Wear coefficient values (using Rockwell Hardness B) versus normal load (36 scratches, 108 profiles)

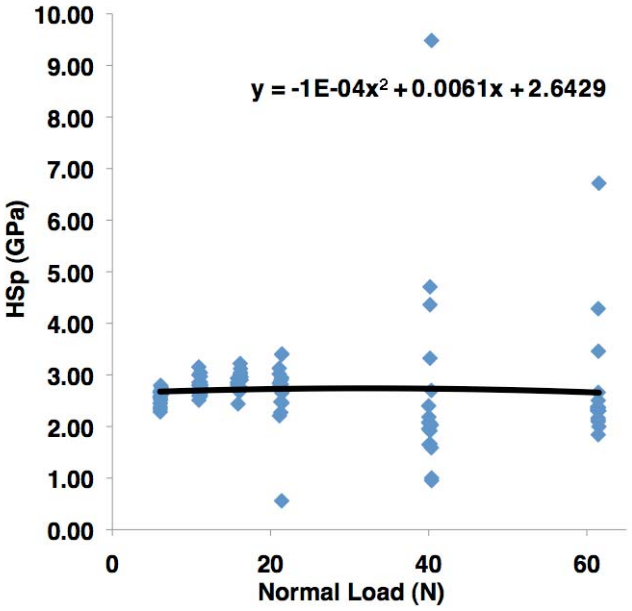

Figure 17. Scratch hardness number versus applied normal load (36 scratches, 108 profiles)

EVALUATION / RECOMMENDATIONS

By reviewing the lunar dust issues known to have occurred during the Apollo missions and identifying key contamination points on future spacesuit of spacecraft designs, specific modes of wear can be identified and defined for investigation. The two main modes of dust interactions occur when spacecraft, spacesuit, or robotic materials either comes into direct contact with the lunar surface or dust is present between two adjacent surfaces. Examples are listed in Figure 18 and Figure 19. It should be noted, however, that wear could be occurring on all materials involved. Under categorization of wear, sliding and rolling are considered non-abrasive wear [24], but for the purposes of defining interactions, rolling also coincides with rotation.

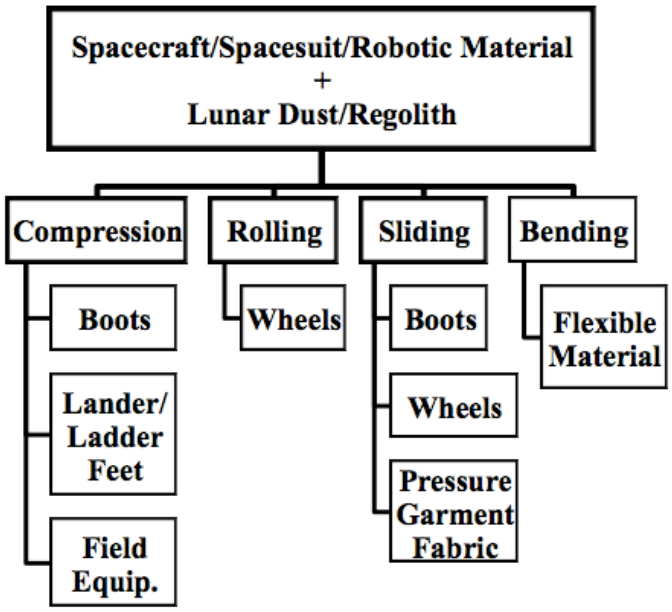

Figure 18. Materials interacting directly with lunar dust

Although Figure 19 addresses interactions with two similar or different space construction materials interacting with dust, fundamentally it can be viewed as dust interacting independently on each surface with an applied force. With this reasoning, it would not be necessary to test multiple materials in the same abrasion test; rather, the results can be extended toward applications or scenarios that include two or more materials interfacing with dust.

With the different abrasion-modes, relevant tests can be developed, which will be either a two-body or three-body apparatus. Wear properties of lunar dust simulant or lunar minerals can be measured versus commonly employed lunar spacecraft, spacesuit, and robotic construction materials. The type of measurements will depend on the test configuration but will include common practices of mass changes, volume loss measurements, and surface deformation. As abrasion simulations are conducted, the data can be used to predict a relationship between the lunar simulants and actual dust.

The limitations of this method are being investigated. The primary concern for the data obtained is the consistency of the scratch tester motor speeds. The higher the applied normal load force, the shorter the final scratch length. This is assumed to be an artifact of the power provided to the motors and will need to be addressed in future analysis.

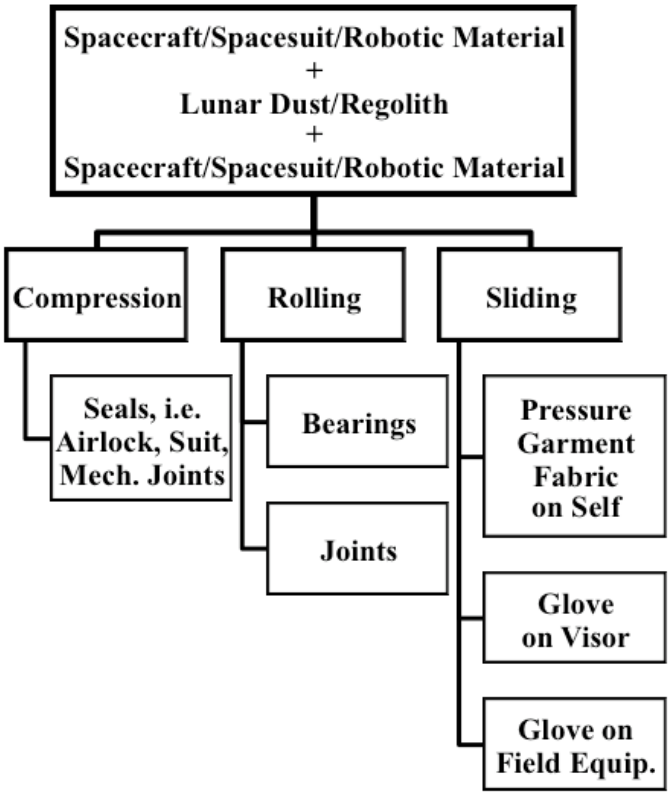

Figure 19. Materials interacting with lunar dust between them

Insight into these potential abrasive impacts on the hardware will influence material selection for a given application. Results from this analysis can then be used in future design trade studies and sensitivity analyses.

Recommendations from this process will also feed back into improving lunar simulant design or test procedures. An additional outcome from characterizing the simulant properties would be to update their corresponding Figures of Merit (FoM). NASA Marshall Space Flight Center has developed a computer program to complement the available simulant data. The FoM software provides guidelines for testing and confidence intervals for how well a simulant compares to regolith for a limited number of physical properties, which could be expanded to include abrasion.

FUTURE WORK

Three-body testing is being investigated to measure interactions with bulk materials on surfaces to compliment this two-body abrasion research. Upcoming test plans with Bud Labs, Inc. are outlined in Table 2. JSC-1a has been the lunar simulant used by investigators, which represents the lunar mare. LHT is being developed by the USGS as a representative simulant of the lunar highland regions. The sand selected is used in ASTM G65 and the alumina is used in ASTM G76.

Table 2. Three-body low/high stress (LS/HS) abrasion testing plans

Abraded Material	Abrasive	Size	Batch
PMMA	JSC-1a	Nominal 30 μm	1
1045 Steel	JSC-1a	Nominal 30 μm	1
6061 Al	JSC-1a	Nominal 30 μm	1
PMMA	Alumina	50 μm avg. dia.	1
1045 Steel	Alumina	50 μm avg. dia.	1
6061 Al	Alumina	50 μm avg. dia.	1
PMMA	Sand	50/70 mesh	1
1045 Steel	Sand	50/70 mesh	1
6061 Al	Sand	50/70 mesh	1
PMMA	JSC-1a	< 30 μm	2
1045 Steel	JSC-1a	< 30 μm	2
6061 Al	JSC-1a	< 30 μm	2
PMMA	LHT Glass	TBD	3
1045 Steel	LHT Glass	TBD	3
6061 Al	LHT Glass	TBD	3

Planned upcoming tasks in this ongoing study include:

- Custom tip fabrication of lunar minerals and scratch testing;
- Data analysis of custom tips;
- Normalization investigation relating tip geometry to applied normal load;
- Correlation development for material properties and abrasion results;
- Submission of updates to ASTM standards on two-body abrasion scratch testing;
- Additional materials and surface coatings/finishes to be tested with various tips; and
- Applying the results to material selection and mission design in terms of modes of lunar dust interactions.

CONCLUSION

The overall research goals of this lunar dust abrasion study include improving the fidelity and repeatability of scratch test analyses; developing simple, robust scratch measuring and standard ranking techniques; and correlating wear parameters to candidate system design applications. Furthermore, these test results provide a foundation from which statistical ‘significance’ from data analysis of controlled, single scratches can be extended toward characterizing ‘meaningfulness’ of the results in terms of integrated hardware performance under lunar environmental conditions. As such, the test outcomes translate to cost saving benefits. By assisting designers in selecting appropriate construction materials for surface systems, based on their intended application and specific location, operational dependability and lifetime can be optimized for safe and efficient future exploration of the Moon.

ACKNOWLEDGMENTS

This research is supported by a NASA Graduate Student Researchers Program (GSRP) grant (NNX07AR55H). MATLAB assistance was provided by Kevin Higdon, Ph.D. Candidate (CU-Boulder). SEM work was conducted by Prof. Sayed M. Khalil (Sohag University, Egypt) at the Nanomaterials Characterization Facility, CU-Boulder. NASA support for this GSRP research effort was provided by the Dust Management Project, under the Exploration Technology Development Program. Test equipment and support were provided by NASA Glenn Research Center. Additional support was provided by BioServe Space Tech. (CU-Boulder).

REFERENCES

1. NASA (2004): “The Vision for Space Exploration”. NASA Headquarters, Washington DC, FEB 2004, NP-2004-01-334-HQ.
2. Volosin, J. (2006): “Dawn of a New Space Age: Developing a Global Exploration Strategy”. Presentation, AIAA’s 2nd Space Exploration Conference, Houston, TX, 6 Dec. 2006.
3. Culbert, C. (2008): “Lunar Surface Systems”. Presentation, AIAA’s 3rd Space Exploration Conference, Denver, CO, 26 Feb. 2008.
4. Kobrick, R.L., Street, K.W., Klaus, D.M., Greenberg, P.S. & Hyatt, M.J. (2008): “Developing Abrasion Testing Hardware to Evaluate Effects Caused by Lunar Dust on Construction Materials”. 59th International Astronautical Congress. Space Exploration Symposium, Interactive Session on Moon Exploration, IAC-08-A3.2.INT3, Glasgow, UK.
5. Gaier, J.R. (2007): “The Effects of Lunar Dust on EVA Systems During the Apollo Missions”. NASA, Glenn Research Center, Cleveland, OH. NASA/TM-2005-213610/REV1.
6. Taylor, L.A., Schmitt, H.H., Carrier, W.D. & Nakagawa, M. (2005): “The Lunar Dust Problem: From Liability to Asset,” AIAA 1st Space Exploration Conference: Continuing the Voyage of Discovery. Orlando, FL. AIAA 2005-2510.
7. Rickman, D. & Street, K.W. (2008): "Expected Mechanical Characteristics of Lunar Dust: A Geological View". Proceedings of the Space Technology and Applications International Forum, Albuquerque, NM, 12 Feb 2008.
8. Plescia, J. (2008): “Lunar Regolith Formation and Properties”. Presentation, Lunar Regolith Community of Practice (LunRCoP) Webinar, 26 Feb 2008.
9. Colwell J. E., Batiste S., Horányi M., Robertson S. & Sture S. (2007): “Lunar surface: Dust dynamics and regolith mechanics”. Rev. Geophys., 45, RG2006, doi:10.1029/2005RG000184.
10. Heiken, G.H., Vaniman, D.T., French, B.M. (1991): “LUNAR Sourcebook: A User’s Guide to the Moon”. Cambridge University Press and Lunar and Planetary Institute.
11. Phillips, T. (2006): “Apollo Chronicles: The Mysterious Smell of Moondust”. Featured online at Science@NASA, 30 Jan 2006. Accessed 25 May 2006, URL: http://science.nasa.gov/headlines/y2006/30jan_smellofmoondust.htm
12. Mitchell, J.K., Houston, W.N., Scott, R.F., Costes, N.C., Carrier, III, W.D. & Bromwell, L.G. (1972): “Mechanical properties of lunar soil: Density, porosity, cohesion, and angle of internal friction”. Proceedings of the Third Lunar Science Conference (Supplement 3, Geochimica et Cosmochimica Acta) Vol. 3, pp 3235-3253.
13. ASTM (1997): “Friction and wear testing: source book of selected references from ASTM Standards and ASM Handbooks”. ASTM & ASM International, West Conshohoken, PA & Materials Park, OH.
14. Budinski, K.G. & Ives, L.K. (2005): “Measuring abrasion resistance with a fixed abrasive loop”. Wear, 258, pp 133-140.
15. ASTM (2005): “Standard Terminology Relating to Wear and Erosion”. G 40-05, Annual Book of ASTM Standards, ASTM.
16. Rabinowicz, E. (1995): “Friction and wear of materials, 2nd Edition”. New York: Wiley.
17. ASTM (2003): “Standard Test Method for Scratch Hardness of Materials Using a Diamond Stylus”. G 171-03, Annual Book of ASTM Standards, ASTM.
18. Westbrook, J.H. & Jorgensen, P.J. (1968): “Effects of Water Desorption on Indentation Microhardness Anisotropy in Minerals”. The American Mineralogist, Vol. 53, pp. 1899-1909.
19. Tabor, D. (1970): “The hardness of solids”. Review of Physics in Technology 1, pp. 145-79.
20. Jiang, J., Sheng, F. & Ren, F. (1998): “Modelling of two-body abrasive wear under multiple contact conditions”. Wear, 217, pp. 35-45.
21. Hamblin, M.G. & Stachowiak, G.W. (1995): “A multi-scale measure of particle abrasivity, and its relation to two-body abrasive wear”. Wear, 190, pp 190-196.
22. Davis, J.R., Allen, P., Lampman, S.R., Zorc, T.B., Henry, S.D., Daquila, J.L. & Ronke, A.W. (1993): “Metal Handbook, Tenth Edition, Volume II, Properties and Selection: Nonferous Alloys and Special-Purpose Materials”. ASM International, Metals Park, OH.
23. Coleman, H.W. & Steele, W.G. (1999): “Experimentation and Uncertainty Analysis for Engineers, Second Edition”. IEEE, New York: Wiley.
24. Budinski, K.G. (2007): “Guide to Friction, Wear, and Erosion Testing”. ASTM International, West Conshohocken, PA. MNL56.

CONTACT

The contact author, Ryan L. Kobrick, is a Ph.D. Candidate in the Aerospace Engineering Sciences Department at the University of Colorado at Boulder (Kobrick@colorado.edu).